City Research Online

City, University of London Institutional Repository

Journal Pre-proof

Distinct processing of aversive experience in amygdala subregions

Jochen Michely, Francesco Rigoli, Robb B. Rutledge, Tobias U. Hauser, Raymond J. Dolan
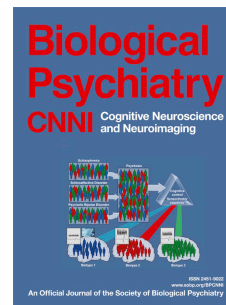
Please cite this article as: Michely J., Rigoli F., Rutledge R.B., Hauser T.U. & Dolan R.J., Distinct processing of aversive experience in amygdala subregions, *Biological Psychiatry: Cognitive Neuroscience and Neuroimaging* (2019), doi: https://doi.org/10.1016/j.bpsc.2019.07.008.

This is a PDF file of an article that has undergone enhancements after acceptance, such as the addition of a cover page and metadata, and formatting for readability, but it is not yet the definitive version of record. This version will undergo additional copyediting, typesetting and review before it is published in its final form, but we are providing this version to give early visibility of the article. Please note that, during the production process, errors may be discovered which could affect the content, and all legal disclaimers that apply to the journal pertain.

Distinct processing of aversive experience in amygdala subregions

Jochen Michely[1,2], Francesco Rigoli[1,3], Robb B. Rutledge[1,2],

Tobias U. Hauser[1,2], Raymond J. Dolan[1,2]

[1] Wellcome Centre for Human Neuroimaging, University College London, London, United Kingdom

[2] Max Planck UCL Centre for Computational Psychiatry and Ageing Research, University College London, London, United Kingdom

[3] City, University of London, Northampton Square, London, United Kingdom

Running title: Amygdala subregions in aversive experience

Corresponding Author: Jochen Michely, Wellcome Centre for Human Neuroimaging,
University College London, London WC1N 3AR, United Kingdom,
Phone number: +44 (0)20 3448 4362; Email: j.michely@ucl.ac.uk

Keywords: threat | anxiety | fMRI | basolateral amygdala | centromedial amygdala | emotional processing

Abstract

Background: The amygdala is an anatomically complex medial temporal brain structure whose subregions are considered to serve distinct functions. However, their precise role in mediating human aversive experience remains ill understood.

Methods: We used functional MRI in 39 healthy volunteers with varying levels of trait anxiety to assess distinct contributions of the basolateral (BLA) and centromedial amygdala (CMA) to anticipation and experience of aversive events. Additionally, we examined the relationship between any identified functional subspecialisation and measures of subjective reported aversion and trait anxiety.

Results: Our results show that the CMA is responsive to aversive outcomes, but insensitive to predictive aversive cues. In contrast, the BLA encodes an aversive prediction error that quantifies whether cues and outcomes are worse than expected. A neural representation within the BLA for distinct threat levels was mirrored in self-reported subjective anxiety across individuals. Furthermore, trait-anxious individuals were characterised by indiscriminately heightened BLA activity in response to aversive cues, irrespective of actual threat level.

Conclusions: Our results demonstrate that amygdala subregions are distinctly engaged in processing of aversive experience, with elevated and undifferentiated BLA responses to threat emerging as a potential neurobiological mediator of vulnerability to anxiety disorders.

Introduction

Fear and anxiety are adaptive responses to demands of everyday life, such as environmental threat. When these aversive responses are exaggerated, they may lead to a range of anxiety disorders (1). However, it remains unclear why human subjects differ so strikingly in their subjective response to objectively similar threats, and in turn in the expression of anxiety traits (2).

The amygdala is a key structure for processing aversive experience and negative emotional information (3, 4). Previous research has highlighted its relevance for threat processing, ascribing to it a role in the genesis of disorders that encompass the anxiety spectrum (5, 6). The amygdala is anatomically heterogeneous, with distinct subregions assumed to serve different functional roles (7). At least two major functional subregions can be identified, the basolateral (BLA) and centromedial (CMA) amygdala (8, 9).

Despite substantial evidence derived from non-human animal experiments (10) and human anatomical studies (11, 12), little is known regarding a functional subspecialisation within human amygdala nuclei (13). Recent neuroimaging studies suggest that CMA and BLA might have distinct functional roles in humans, primarily in the context of associative learning (14, 15), threat prioritisation (16), and social functioning (17, 18).

However, how human amygdala subregions process aversive events, and how expectations about these events modulate these functions, remains unknown. Moreover, due to the fact that subjective experience cannot be assessed in non-human animal models, it remains elusive how amygdala subregions mediate a transformation from objective threat to subjective aversion. Thus, the goal of our study was two-fold: Firstly, we combined functional MRI with a novel Pavlovian conditioning paradigm to probe the exact roles of BLA and CMA in threat processing, i.e., aversive expectation. Secondly, we assessed how

3

both interindividual and trial-by-trial variability in aversive signals in the amygdala relate to both subjective and trait anxiety. Given its substantial sensory afferent information and implication in threat processing in non-human animals, we hypothesized BLA, but not CMA, to encode threat expectations (19, 20). Moreover, we conjectured such a neural signature of threat within BLA to be related to interindividual differences in anxiety traits (21). Ultimately, due its role as the major amygdala output centre and in the generation of responses to acute stressors such as pain (22-24), we assumed CMA activity in response to aversive events to be reflected in subjective reports of aversion.

Methods and Materials

Participants

42 healthy, right-handed volunteers (screened for neurological and psychiatric conditions, including anxiety disorders and phobias) participated in this experiment and received monetary compensation for their time (£30-£40). Participants were recruited along usual guidelines from an online subject pool at University College London (UCL), but not through courses or lectures given by the authors. Data from three subjects were excluded due to equipment failure involving electrical stimulation during scanning, leaving 39 participants for all subsequent behavioural and neural analyses (mean age: 25.0; range 18-39 years; 22 females). The experimental protocol was approved by UCL research ethics committee, informed consent was obtained from all participants.

Trait anxiety

To measure trait anxiety, subjects filled out the Spielberger State-Trait Anxiety Inventory (STAI) trait subscale after the scan, a self-report questionnaire of high internal

consistency (Cronbach's alpha in present sample: $\alpha=0.92$) that is commonly used to measure anxiety in clinical and non-clinical samples (25, 26). The score ranges between 20 and 80, with higher scores indicating greater trait anxiety.

Experimental task

We aimed to characterise how participants anticipate and process aversive events (painful electric shocks to the hand), and how neural signals in response to threat relate to subjective experience and trait anxiety. To this end, we designed a novel task consisting of 180 trials, divided into four blocks of 45 trials each.

On each trial, subjects were presented with a picture of an insect, either a mosquito or a bug, shown next to the back of an image of a hand for 4000ms. Each insect signalled a specific probability of receiving an electrical shock, with one insect (*high* probability cue, 90 trials) followed by a shock on 70% of trials (63 shocks) and by no shock 30% of trials, and the other insect (*low* probability cue, 90 trials) followed by a shock on 30% (27 shocks), and no shock on 70% of trials (insects were counterbalanced across subjects). Note that cues were perfectly matched with respect to their uncertainty (absolute deviation from probability of shock equal to 50%), differing solely in objective predictiveness of shock receipt.

To avoid any influence arising out of learning, subjects were familiarised with shock probability attributed to each stimulus in a pre-scanning training and explicitly informed that probabilities remained fixed throughout the entirety of training and experiment. Outcome onset was indicated by appearance of a red dot (duration: 1500ms), either displayed next to the hand (indicating no shock) or superimposed on the hand (indicating shock, shock duration: 100ms). If the red dot was displayed on the hand, shocks were applied simultaneous in time to its appearance.

After a jittered fixation cross (mean: 3000ms; uniformly distributed between 1500-4500ms), subjects were asked to rate their anticipatory anxiety using a slider ("How anxious did you feel while the insect was present?"). Importantly, subjects were instructed and previously trained to recall the subjective state/feelings elicited by predictive cue presentation, ignoring the actual outcome of each trial. Ratings were given without time restrictions by moving a cursor (always starting at the midpoint) along a scale that spanned "not anxious" on the extreme left through to "very anxious" on the extreme right. After another jittered fixation (mean: 3000ms; range: 2000–4000ms), the appearance of hand and insect indicated beginning of the next trial.

On average, one block lasted 11min, with minor variation between subjects depending on times for self-paced anxiety ratings. Between blocks, subjects were allowed a break, and we repeated a short pain titration procedure (see below for details). Overall, the task in the scanner lasted on average 55min.

Electrical stimulation

Participants underwent an individually tailored pain titration procedure (27, 28) with a Digitimer DS7a electric stimulator (Welwyn Garden City, UK) that can produce stimulator output as high as 100mA. An electrode was placed on the back of the subject's left hand and titration began with a low-current electric shock (0.1 mA), where subjects were asked to rate its painfulness on a visual 21-point scale (ranging from 0='not unpleasant' to 5='quite unpleasant' to 10='extremely unpleasant and unbearable'). For each subsequent shock, intensity was increased in small increments with subject's approval. This procedure was repeated until subjective ratings of pain reached 7 ('very unpleasant but bearable'). This intensity was used for the first block of the experiment. To avoid excessive habituation to stimulation, and excessive pain due to increased shock sensitivity over the course of the

experiment, a short titration procedure was repeated within the scanner before each of the four experimental blocks. Hence, perceived subjective experience was kept constant throughout the experiment. Mean shock intensity across subjects was 2.3mA ± 1.3 (range 0.5-6.7), and there was no relationship between chosen intensity and trait anxiety (r=-0.094, p=0.569).

Pre-scanning training

Subjects performed two practice blocks (20 trials each) outside the scanner. This ensured they had learned the two levels of shock probability and familiarized themselves with the task structure. Importantly, subjects were informed beforehand that one of the insects would be associated with a high and the other with a low chance of predicting an upcoming shock.

Whilst the first block familiarized subjects with stimuli and associated shock probabilities, i.e., without provision of subjective ratings, the second block was the same as in the scanner, including subjective ratings. Analysis of the second training block indicated that subjects had learned to dissociate the two threat stimuli before entering the scanner, as indicated by a strong difference in anxiety ratings for high versus low threat stimuli (Supplementary Fig. 1).

fMRI data acquisition and preprocessing

T2*-weighted echo-planar imaging (EPI) MRI data was acquired using a Siemens Trio 3T scanner, using a 32-channel head coil. We collected whole-brain data, 42 slices with 3mm isotropic voxels; repetition time (TR): 2.94s; echo time (TE): 30ms; slice tilt: −30° (T>C) relative to scanner axis; Z-shim -0.4. This sequence is designed for optimal sensitivity and reduced susceptibility-induced signal dropout particularly in temporal regions such as

amygdala (29). To account for T1-saturation effects, the first six volumes of each session were discarded. Additionally, whole-brain field maps (3mm isotropic, 10ms/12.46ms TE for short/long respectively, 37ms total EPI readout time, phase-encode blip polarity −1) were acquired to correct EPIs for field strength inhomogeneity. All fMRI analyses were performed using default settings within SPM12 (Wellcome Centre for Human Neuroimaging; www.fil.ion.ucl.ac.uk). EPIs were realigned and unwarped using the field maps, subsequently co-registered to subject-specific anatomical images and normalised to MNI-space, using the 1.5mm MNI152 atlas implemented in SPM12. Finally, normalized EPIs were smoothed with a 6mm FWHM-kernel to satisfy smoothness assumptions of statistical correction algorithms. To ascertain these results were robust, we conducted additional analyses using reduced smoothing kernels (4.5mm, 3mm), which yielded similar results (Supplementary Table 1).

Structural MRI data acquisition

Structural images were acquired using quantitative multiparameter maps (MPMs) in a 3D multi-echo fast-low angle shot (FLASH) sequence with 1-mm isotropic resolution (30). Three different FLASH datasets were acquired: predominantly MT weighting (TR/α = 23.7ms/6°; excitation preceded by an off-resonance Gaussian MT pulse of 4ms duration, 220° nominal flip angle, 2 kHz frequency offset), proton density weighting (PD; = 23.7ms/6°), and T1 weighting (18.7ms/20°). To increase signal-to-noise ratio, signals of six equidistant bipolar gradient echoes (echo time 2.2-14.7ms) were averaged. Semiquantitative MT maps were calculated using mean signal amplitude and T1 maps (31), additionally eliminating influence of B1 inhomogeneity and relaxation effects (32).

Behavioural analysis

To assess what influenced subjects' anxiety ratings, we ran an ANOVA with factors 'expectation' (high/low) and 'outcome' (shock/no shock).

Additionally, we fitted a trial-by-trial linear regression model. To predict anxiety ratings on current trial T, we used (i) probability (high vs. low), (ii) outcome type (shock vs. no shock), and (iii) interaction term, (iv) elapsed time between outcome offset and rating onset, (v) rating time (from ratings onset to offset), whilst also testing for influence of (iv & v) outcome type of previous trials, i.e., trial T-1 and T-2.

Behavioural analyses were conducted in Matlab (version 2016, The MathWorks) and SPSS (version 25, IBM).

fMRI analysis

The main goal of our fMRI analysis was to characterise how different amygdala subregions respond to aversive states, i.e., anticipation and experience of negative outcomes. In a General Linear Model (GLM), we entered two different regressors at time of cue, for high and low probability of upcoming shock, respectively. At time of outcome, we entered four regressors, separating high expectation shock, high expectation no shock, low expectation shock, and low expectation no shock. Additionally, we entered four equivalent regressors at time of subjective rating period onset. In order to examine how amygdala responses at the actual time of rating relate to subjective anxiety ratings on a trial-by-trial basis, we used parametric modulators containing trial-by-trial ratings for each regressor, i.e., each condition separately. Hence, we assessed the relationship between amygdala activity and subjective reports irrespective of the condition that subjects were in.

Note that first-level regressors were modelled as events, i.e., 0sec duration, and convolved with SPM's canonical hemodynamic response function as in previous studies assessing amygdala activity in event-related designs (e.g., 15, 26, 33). We regressed out

movement-related variance using six head motion parameters as assessed by the realignment algorithm. Each run was modelled as separate session to account for offset differences in signal intensity.

To assess activity in amygdala subregions we used cytoarchitectonically demarcated probabilistic maps, focusing specifically on centromedial (CMA; central and medial nuclei) and basolateral (BLA; lateral, basolateral, basomedial, and paralaminar nuclei) nuclear groups (34). Masks were created via the SPM anatomy toolbox, i.e., cytoarchtectonically defined by using maximum probability maps, representing summary maps of different probabilistic cytoarchitectonic maps (34, 35). One of the advantages of these maps is that they allow the definition of a continuous volume for a subregion without any overlap with other subregions. Another advantage is that the procedure accords with existing fMRI studies on human amygdala subspecialisation using similar methods (e.g., 15, 33, 36, 37). We refer to this parcellation as CMA and BLA masks in the results section (cf. Supplementary Fig. 2 for detailed visualisation of the masks).

To demonstrate the robustness of task-activated amygdala responses without the restrictions of a parcellation approach, we also used a bilateral anatomical mask for the entire amygdala from the WFU PickAtlas toolbox in SPM, defined by using the Automated Anatomical Labelling (AAL) atlas. We refer to this independent mask as 'entire amygdala' in the results section. To correct for multiple comparisons, we used a family-wise error (FWE) rate threshold of $p<0.05$, small volume corrected for predefined bilateral regions of interest (uncorrected height threshold $p<0.001$). Figures of whole-brain maps at the respective height threshold are presented in Supplementary Fig. 6. Additionally, we report activations surviving at $p<0.05$ FWE-corrected for the whole brain. Activations are reported using x, y, z coordinates in MNI-space.

Results

Retrospective anxiety as function of actual threat and experienced outcomes

To assess how objective threat is transformed into the subjective experience of anxiety, we asked subjects to report how anxious they felt during predictive cue presentation, i.e., before outcomes were revealed. Importantly, we probed subjects after outcome delivery by specifically asking for a subjective judgement about feelings at cue presentation. As per instruction, these self-reports should not be influenced by actual outcomes. We ran an ANOVA with factors 'expectation' (high/low) and 'outcome' (shock/no shock). This revealed significant main effects of 'expectation' [$F(1,38)=103.505$, $p<0.001$] and 'outcome' [$F(1,38)=24.430$, $p<0.001$], with no interaction [$F(1,38)=2.153$, $p=0.151$]. An additional trial-by-trial linear regression model confirmed these results whilst additionally showing no effect of outcome history, elapsed time since outcome receipt, or time taken to report (Supplementary Fig. 3). Importantly, a separate analysis of the 1st and 2nd half of the experiment indicated that anxiety ratings were remarkably stable across halves (Supplementary Fig. 1). Findings indicate anxiety ratings were strongly influenced by both objective threat level, i.e., greater for high vs. low expectation of upcoming shock, and biased by experienced outcomes, i.e., greater for shock vs. no shock trials. Thus, subjects not only dissociated between objectively different threat levels at cue, but their subjective reports of anxiety were distorted by a recent receipt of an aversive outcome.

Threat dissociation during aversive anticipation in BLA

To investigate how amygdala subregions responded to objective threat we used a voxel-based analysis, comparing cue-elicited responses signalling high vs. low probability of upcoming shocks. The BLA showed a significant dissociation for threat levels, with a significantly enhanced response to high compared to low shock probability cues (Fig. 2A; [29 3 -24], t(38)=4.47, P_{FWE}=0.018 BLA, P_{FWE}=0.028 entire amygdala). A control analysis using a finite impulse response set showed a remarkably similar result (Supplementary Figure 4), confirming that BLA threat response was accurately modelled using a canonical hemodynamic response function. We did not find such threat level modulation in CMA (even at an uncorrected height threshold of p<0.001), suggesting a functional dissociation with only BLA processing threat.

To formally assess a dissociation in responsivity across subregions, we compared mean activation at cue for both subregions. For this analysis, we extracted average beta values across all voxels within bilateral anatomical masks. A rm-ANOVA, with factors 'subregion' (BLA/CMA), 'expectation' (high/low), showed no effect of subregion [F(1,38)=0.094, p=0.760], a statistical trend for expectation [F(1,38)=3.209, p=0.081], and a trend-level interaction [F(1,38)=3.379, p=0.074]. Follow-up t-tests showed BLA responses were greater for high as compared to low probability of upcoming shock (t(38)=2.504, p=0.017), whilst no such effect evident in CMA (t(38)=0.932, p=0.357; Fig. 2B). These results suggest the BLA shows a modulation in response across threat levels during anticipation of aversive outcomes.

Dissociable response in BLA and CMA to aversive outcomes

The amygdala represents aversive outcomes, and these responses are thought to be modulated by expectation (15, 38). Thus, we asked how BLA and CMA respond to aversive events and whether there was a modulation by expectation related to these same events. We first compared activity for shock versus no shock outcomes, irrespective of prior expectation. A voxel-based analysis revealed significant activation in the amygdala, with bilateral peaks centred on CMA (Fig. 3A; [-20 -6 -12], t(38)=7.20 & [26 -9 -12], t(38)=7.07, P_{FWE}<0.001 CMA, P_{FWE}<0.001 entire amygdala). Significant shock responses were also found in bilateral BLA ([26 3 -21], t(38)=5.83, P_{FWE}<0.001 BLA; [-24 -2 -20], t(38)=4.79, P_{FWE}=0.007 BLA). Extending this analysis to the whole brain, we found areas encompassing a so-called 'pain matrix' responding more to shocks than no shock conditions (Supplementary Fig. 5 & Table 3; including bilateral insula, adjacent somatosensory cortex, medial/anterior cingulate cortex, periaqueductal gray, thalamus, and amygdala; p<0.05 whole-brain FWE-corrected). To assess whether head motion could account for neural shock signals, we assessed framewise displacement (FD) during our task. Here, the comparison of FD for shock vs. no shock period showed no difference (1 volume post outcome onset: p=0.581, 3 volumes: p=0.206, 5 volumes: p=0.400). Thus, head movements during shock delivery did not account for these findings.

Next, we assessed whether expectation modulated outcome processing. We found an expectation effect on BLA responses to outcomes (Fig. 3B; [-26 -2 -30], t(38)=4.44, P_{FWE}=0.020 BLA, P_{FWE}=0.016 entire amygdala), with greater activation for low versus high expectation trials. Such an expectation-induced effect was not evident in CMA. This suggests while both subregions respond to shock, the BLA alone encodes an expectation of shock outcomes.

To assess this functional dissociation more formally, we examined mean activation for all four outcome types within bilateral anatomical masks (Fig. 3C&D). A rm-ANOVA

with factors 'subregion' (BLA/CMA), 'expectation' (high/low), 'outcome' (shock/no shock) showed an effect of subregion [$F_{(1,38)}=5.614$, $p=0.023$] and outcome [$F_{(1,38)}=24.652$, $p<0.001$], but no effect of expectation [$F_{(1,38)}=2.182$, $p=0.148$]. We identified a significant interaction between subregion and expectation [$F_{(1,38)}=10.082$, $p=0.003$], and between subregion and outcome [$F_{(1,38)}=43.206$, $p<0.001$]. Post-hoc t-tests confirmed that whilst both subregions responded significantly to shock (BLA: $t_{(38)}=3.167$, $p=0.003$; CMA: $t_{(38)}=5.965$, $p<0.001$; Fig 3E), this response was significantly greater in CMA than BLA ($t_{(38)}=6.573$, $p<0.001$). In contrast, BLA alone encoded expectation (BLA: $t_{(38)}=3.169$, $p=0.003$; CMA: $t_{(38)}=-0.144$ $p=0.886$; Fig. 3E), indicated by a significant interaction between subregion and expectation, reflecting an effect greater for BLA than CMA ($t_{(38)}=3.175$, $p=0.003$). There was no significant three-way interaction [$F_{(1,38)}=0.003$, $p=0.956$], indicative of the two-way interactions representing two separate effects.

Overall, the profile of BLA response fulfilled requirements for a signed aversive prediction error (39), with enhanced response for less compared to highly predicted aversive events ($t_{(38)}=2.343$, $p=0.024$), and an attenuated response for less as compared to a highly predicted aversive event omission ($t_{(38)}=2.232$, $p=0.032$; Fig. 3D).

Amygdala activity and subjective aversive experience

As highlighted above, retrospective reports of cue-elicited anxiety were influenced by both objective threat level at cue and by outcomes (Fig. 4A). Consequently, we asked how amygdala activity in response to threat and aversive outcomes related to reports of aversive experience. Firstly, we examined whether the neural dissociation between threat levels in BLA at cue related to a corresponding effect of expectation on self-reported anxiety. We found that threat-related modulation of BLA activity (high vs. low objective probability of upcoming shock) correlated with an equivalent dissociation of threat levels in subjective

reports (high vs. low objective probability of shock, peak voxel activity; Fig. 4B; r=0.373, p=0.020). Notably, this relationship remained significant when controlling for CMA activity (r=0.357, p=0.028). However, there was no such relationship for CMA activity alone (r=0.113, p=0.491). This indicates that greater threat-related modulation of BLA activity is mirrored in a behavioural dissociation of threat-induced subjective anxiety across participants.

Next, we assessed whether shock effects at outcome as observed in both BLA and CMA related to corresponding distorting outcome effects on retrospective anxiety reports. We found no significant relationship (shock vs. no shock, peak voxel activity: CMA: r=0.076, p=0.645; BLA: r=0.101, p=0.542), indicating no systematic impact of amygdala shock responses and subjective reports across participants.

Finally, we tested whether amygdala responses at the actual time of rating, i.e., when aversive experience was retrospectively constructed related to how anxious subjects reported to have felt. Importantly, we here used a separate parametric modulator for each of the four conditions at rating period onset. Thus, we regressed out main effects of cues and outcomes so as to control for the known impact of expectation and shock, assessing the relationship between amygdala activity and subjective reports irrespective of the condition that subjects were in. CMA activity positively correlated with subjective anxiety reports (Fig. 4C; [-23 -6 -12], t(38)=4.14, P_{FWE}=0.011 CMA, P_{FWE}=0.032 entire amygdala). There was no such effect in BLA. A rm-ANOVA with factors 'subregion' (BLA/CMA), 'expectation' (high/low), 'outcome' (shock/no shock) to confirm a functional subspecialisation showed an effect of subregion [F(1,38)=6.700, p=0.014] and a significant subregion outcome interaction [F(1,38)=8.068, p=0.007]. Follow-up t-tests confirmed a significant effect in CMA (t(38)=2.232, p=0.032), but not BLA (t(38)=0.512, p=0.611, Supplementary Fig. 7).

Moreover, the effect was significantly greater in CMA than BLA (t(38)=2.588, p=0.014), particularly after shock as compared to no shock outcomes (t(38)=2.841, p=0.007).

This suggests post-shock CMA activity when making retrospective anxiety reports, i.e., after outcomes were revealed, biased the recollected subjective experience of previous anticipatory aversive states.

Threat signals in BLA relate to trait anxiety

Previous research has reported amygdala hyperactivity in highly anxious individuals across a range of experimental paradigms (40-42). However, the exact relationship between amygdala responses to threat and trait anxiety remains unclear. One hypothesis proposes anxious individuals do not regulate amygdala responses to variable levels of threat, thus exhibiting indiscriminately heightened amygdala activation (43-45).

To specifically test this hypothesis, we correlated a BLA response that encoded objectively different threat levels with trait anxiety scores. We found that a greater neural dissociation between cue-elicited BLA responses (high vs. low probability of upcoming shock, peak voxel activity) was significantly associated with lower trait anxiety (Fig. 5B; r=-0.322, p=0.045). Notably, this relationship remained significant when controlling for CMA activity (r=-0.383, p=0.018). However, there was no such relationship for CMA activity alone (r=0.112, p=0.492). This finding supports the notion that trait-anxious individuals are characterized by a reduced discriminatory response to different threat levels in the BLA.

An impaired threat modulation of BLA activity could arise for two reasons. Anxious individuals might fail to activate BLA in response to highly threatening stimuli, or they might display elevated BLA responses to any threatening stimulus, irrespective of its objective threat level. To arbitrate between these explanations, we correlated a BLA response to aversive cues irrespective of threat level (collapsed across high *and* low probability trials,

peak voxel activity) with individual trait anxiety scores. We found a significant positive correlation, i.e., a greater overall cue-elicited BLA response was associated with greater trait anxiety (Fig. 5A; r=0.328, p=0.041). Indeed, there was a positive relationship when testing for low and high threat cues separately (Supplementary Fig. 8). This is in keeping with the idea that highly anxious individuals show heightened BLA activity for aversive cues irrespective of their objective predictability. This suggests trait anxiety is associated with an elevated and undifferentiated threat response in BLA.

Sex differences

The human amygdala is thought to be a sexually dimorphic area (46), and anxiety disorders are more prevalent in women than men (47). Thus, we assessed potential sex differences across our sample of female (n=22) and male (n=17) participants.

Importantly, our sample was matched with regard to age (female: mean 24.5 ± 5.3, male: mean 25.6 ± 5.4; p=0.532) and trait anxiety (female: mean 35.9 ± 7.1, male: mean 34.6 ± 10.7; p=0.647). However, additional analyses (Supplementary Fig. 9) showed that the discrimination for high and low levels of threat in BLA was significantly stronger in females as compared to male participants (t(38)=2.696, p=0.010). Strikingly, this neural dissociation between threat levels showed a highly significant relationship to both subjective anxiety reports during the task (r=0.552, p=0.008) and trait anxiety (r=-0.503, p=0.017) in females, but not male participants (r=-0.082, p=0.753 & r=-0.290, p=0.259). We found no such gender differences for outcome processing or any other comparison of our main results.

This suggest that BLA responsivity to varying levels of threat was particularly pronounced in female individuals, where greater dissociation between high and low levels of

17

threat in BLA was related to greater threat-related dissociation of cues in subjective ratings and lower levels of trait anxiety.

Discussion

We show amygdala subregions, BLA and CMA, are distinctly engaged in processing of aversive experience. Specifically, BLA is engaged by aversive expectations, where a dissociation across threat levels is mirrored by reported subjective anxiety. Importantly, BLA activity relates to trait anxiety, with more anxious subjects showing elevated and undifferentiated responses to threat, an effect particularly pronounced in female individuals. Conversely, CMA responds to aversive outcomes, but is insensitive to aversive cues or their associated expectations.

In many human neuroimaging studies participants are confronted with cues that vary not only in predictability (probability of shock), but also uncertainty (absolute deviation from probability of shock equal to 50%) about upcoming aversive events. For example, previous studies often compared a partially reinforced aversive schedule to stimuli predicting complete safety (e.g., 47-51). This type of design renders it difficult to disentangle effects of predictiveness and uncertainty. Our task allowed us to control for uncertainty and in doing so shows that amygdala subregions play distinct roles in response to predictive stimuli. Most striking here is the observation that BLA activity scales with increasing levels of threat.

The BLA is anatomically well-placed for processing environmental information about potential threat as it receives dense connections from the thalamus and sensory association cortices (37, 52-54). Our findings complement previous accounts of the role of the BLA in learning about threat, demonstrating the BLA is important in detecting variable threat and predicting the occurrence of negative outcomes (15, 19, 20).

Activation in the amygdala to shock was primarily signalled in CMA, highlighting its role in processing acutely imminent threat and pain (22-24). However, in contrast to the CMA, responses to aversive outcomes in the BLA were modulated by expectation, with enhanced activation for less predicted aversive events. This accords with prior neuroimaging studies showing unconditioned response diminution, i.e., reduced responses for expected versus unexpected aversive unconditioned stimuli, in the human amygdala (55,56). Importantly, the BLA also displayed a greater attenuation in responsiveness for less predicted shock omission. Thus, responses at outcome to both aversive events and omission of such events in the BLA have the characteristics of a signed aversive prediction error (39). Such aversive predictions errors are known to play a crucial role in learning from aversive reinforcers such as pain (15, 57, 58). This finding extends on previous studies which have shown the expression of amygdala prediction errors (27, 59) by demonstrating an anatomical specificity to this effect, an observation that is in accord with a similar finding in rodents (60, 61).

Consistent with prior evidence that the amygdala supports interoceptive emotional awareness (21, 62, 63), we found distinct relations of BLA and CMA with subjective experience. A greater neural dissociation within the BLA for threat levels was linked to a threat-related dissociation in reported subjective anxiety across individuals. Intriguingly, fluctuations in CMA activity at time of reporting were linked to subjective experience about previous anxiety states on a trial-by-trial basis. This indicates that retrospective reports about past aversive states are subject to an influence from current representation of outcomes in CMA. This finding aligns with the role of the CMA as the major output centre of the amygdala, in generating behavioural responses to acute stressors (22-24).

An elevated BLA response to aversive cues in highly anxious individuals is consistent with prior neuroimaging findings that suggest a relationship between anxiety and amygdala

hyperactivity (64-68). Importantly, anxious subjects showed a lack of discrimination for variable threat levels in BLA, despite aversive cues being highly predictive. Interestingly, additional analyses showed that the association between greater trait anxiety and blunted threat discrimination in BLA was particularly pronounced in female individuals.

This finding demonstrates that trait-anxious individuals display a failure to regulate BLA activity adequately in response to objectively different threat levels, supporting the notion that anxiety is associated with elevated and undifferentiated amygdala activity, potentially due to a failure to adequately modulate its responses to objective features of the environment (43-45).

This link between a lack of discrimination of BLA responses and trait anxiety also concurs with previous work suggesting trait-anxious individuals do not accurately adjust expectations to reflect changes in environmental contingencies during aversive learning (69, 70). Such a failure to regulate BLA responses might in turn lead to an internal state of uncertainty about threat despite objectively predictable conditions, and to increases in anxiety symptomatology (45, 71). Overall, our findings complement previous studies indicating aberrant threat processing in amygdala putatively playing a role in the onset, or maintenance of anxiety-related disorders (67, 68, 72).

Limitations

Firstly, our study provides multiple layers of evidence for the involvement of BLA but not CMA in responding to threat. However, in contrast to a strong dissociation between subregions for outcome processing, the comparison between subregions for aversive cues only showed a statistical trend. Thus, an involvement of CMA in processing of varying levels of threat cannot be fully ruled out. A second limitation of our study is the limited size and scope of the present sample. Although the observed relations between amygdala activity and

trait anxiety are consistent with prior work (43-45), future studies are needed to assess the reproducibility of these discoveries in larger samples (73, 74). Likewise, it will be fruitful to examine whether these relations extend to individuals with more extreme levels of trait anxiety and to patients meeting diagnostic criteria for anxiety disorder (2).

Conclusion

In conclusion, we show a functional dissociation within the human amygdala in relation to aversive processing. The CMA responds to aversive outcomes, while the BLA represents aversive events and expectations about those events. Moreover, BLA activity scales with increasing levels of threat, with more anxious individuals showing poorer discrimination across distinct threat levels. Our findings provide insight into how human amygdala subregions contribute to subjective anxiety, where an encoding of threat within BLA emerges as a potential neurobiological mediator of vulnerability to anxiety disorders.

Conflict of Interest:

The authors report no biomedical financial interests or potential conflicts of interest.

References

1. Shin LM, Liberzon I (2010) The neurocircuitry of fear, stress, and anxiety disorders. Neuropsychopharmacology 35(1):169-91.

2. Shackman AJ, Tromp DPM, Stockbridge MD, Kaplan CM, Tillman RM, Fox AS (2016) Dispositional negativity: An integrative psychological and neurobiological perspective. Psychol Bull 142(12):1275-1314.

3. Shackman AJ, Fox AS, Oler JA, Shelton SE, Oakes TR, Davidson RJ, Kalin NH (2017) Heightened extended amygdala metabolism following threat characterizes the early phenotypic risk to develop anxiety-related psychopathology. Mol Psychiatry 22(5):724-732.

4. Costafreda SG, Brammer MJ, David AS, Fu CH (2008) Predictors of amygdala activation during the processing of emotional stimuli: a meta-analysis of 385 PET and fMRI studies. Brain Res Rev 58(1):57-70.

5. Oler JA, Fox AS, Shelton SE, Rogers J, Dyer TD, Davidson RJ, Shelledy W, Oakes TR, Blangero J, Kalin NH (2010) Amygdalar and hippocampal substrates of anxious temperament differ in their heritability. Nature 466(7308):864-8.

6. Fox AS, Shackman AJ (2019) The central extended amygdala in fear and anxiety: Closing the gap between mechanistic and neuroimaging research. Neurosci Lett 6;693:58-67.

7. Sah P, Faber ES, Lopez De Armentia M, Power J (2003) The amygdaloid complex: anatomy and physiology. Physiol Rev 83(3):803-34.

8. Freese JL, Amaral DG (2009) Neuroanatomy of the primate amygdala. In: The Human Amygdala. (eds Whalen PJ, Phelps EA), pp. 3–42, New York: The Guilford Press.

9. Yilmazer-Hanke DM (2012) Amygdala. In: The Human Nervous System. (eds Paxinos G, Mai J), pp. 759–834, San Diego, CA: Elsevier.

10. Johansen JP, Cain CK, Ostroff LE, LeDoux JE (2011) Molecular mechanisms of fear learning and memory. Cell 147(3):509-24.

11. Solano-Castiella E, Anwander A, Lohmann G, Weiss M, Docherty C, Geyer S, Reimer E, Friederici AD, Turner R (2010) Diffusion tensor imaging segments the human amygdala in vivo. Neuroimage. 2010 15;49(4):2958-65.

12. Abivardi A, Bach DR (2017) Deconstructing white matter connectivity of human amygdala nuclei with thalamus and cortex subdivisions in vivo. Hum Brain Mapp. 38(8):3927-3940.

13. Terburg D, Scheggia D, Triana Del Rio R, Klumpers F, Ciobanu AC, Morgan B, Montoya ER, Bos PA, Giobellina G, van den Burg EH, de Gelder B, Stein DJ, Stoop R, van Honk J (2018) The Basolateral Amygdala Is Essential for Rapid Escape: A Human and Rodent Study. Cell. 175(3):723-735.

14. Prévost C, McCabe JA, Jessup RK, Bossaerts P, O'Doherty JP (2011) Differentiable contributions of human amygdalar subregions in the computations underlying reward and avoidance learning. Eur J Neurosci 34(1):134-45.

15. Boll S, Gamer M, Gluth S, Finsterbusch J, Büchel C (2013) Separate amygdala subregions signal surprise and predictiveness during associative fear learning in humans. Eur J Neurosci 37(5):758-67.

16. Bach DR, Hurlemann R, Dolan RJ (2015) Impaired threat prioritisation after selective bilateral amygdala lesions. Cortex 63:206-13.

17. Davis FC, Johnstone T, Mazzulla EC, Oler JA, Whalen PJ (2010) Regional response differences across the human amygdaloid complex during social conditioning. Cereb Cortex 20(3):612-21.

18. Gamer M, Zurowski B, Büchel C (2010) Different amygdala subregions mediate valence-related and attentional effects of oxytocin in humans. Proc Natl Acad Sci U S A. 107(20):9400-5.

19. Janak PH, Tye KM (2015) From circuits to behaviour in the amygdala. Nature. 517(7534):284-92.

20. Amir A, Kyriazi P, Lee SC, Headley DB, Paré D (2019) Basolateral amygdala neurons are activated during threat expectation. J Neurophysiol. 121(5):1761-1777.

21. Etkin A, Klemenhagen KC, Dudman JT, Rogan MT, Hen R, Kandel ER, Hirsch J (2004) Individual differences in trait anxiety predict the response of the basolateral amygdala to unconsciously processed fearful faces. Neuron 44(6):1043-55.

22. Fadok JP, Markovic M, Tovote P, Lüthi A (2018) New perspectives on central amygdala function. Curr Opin Neurobiol. 49:141-147.

23. Davis M, Walker DL, Miles L, Grillon C (2010) Phasic vs sustained fear in rats and humans: role of the extended amygdala in fear vs anxiety. Neuropsychopharmacology 35(1):105-35.

24. Veinante P, Yalcin I, Barrot M (2013) The amygdala between sensation and affect: a role in pain. J Mol Psychiatry 5;1(1):9.

25. Spielberger CD, Gorsuch RL, Lushene R, Vagg PR, Jacobs GA (1983) Manual for the State-Trait Anxiety Inventory. Palo Alto, CA: Consulting Psychologists Press.

26. Julian LJ (2011) Measures of anxiety: State-Trait Anxiety Inventory (STAI), Beck Anxiety Inventory (BAI), and Hospital Anxiety and Depression Scale-Anxiety (HADS-A). Arthritis Care Res (Hoboken). 63 Suppl 11:S467-72.

27. Eldar E, Hauser TU, Dayan P, Dolan RJ (2016) Striatal structure and function predict individual biases in learning to avoid pain. Proc Natl Acad Sci U S A 113(17):4812-7.

28. Crockett MJ, Kurth-Nelson Z, Siegel J, Dayan P, Dolan RJ (2014) Harm to others outweighs harm to self in moral decision making. Proc Natl Acad Sci U S A 111(48):17320-5.

29. Weiskopf N, Hutton C, Josephs O, Deichmann R (2006) Optimal EPI parameters for reduction of susceptibility-induced BOLD sensitivity losses: a whole-brain analysis at 3 T and 1.5 T. Neuroimage 33(2):493-504.

30. Weiskopf N, Suckling J, Williams G, Correia MM, Inkster B, Tait R, Ooi C, Bullmore ET, Lutti A (2013) Quantitative multi-parameter mapping of R1, PD(*), MT, and R2(*) at 3T: a multi-center validation. Front Neurosci Jun 10;7:95.

31. Helms G, Dathe H, Dechent P (2008a) Quantitative FLASH MRI at 3T using a rational approximation of the Ernst equation. Magn Reson Med 59:667–672.

32. Helms G, Dathe H, Kallenberg K, Dechent P (2008b) High-resolution maps of magnetization transfer with inherent correction for RF inhomogeneity and T1 relaxation obtained from 3D FLASH MRI. Magn Reson Med 60:1396–1407.

33. Goossens L, Kukolja J, Onur OA, Fink GR, Maier W, Griez E, Schruers K, Hurlemann R. (2009) Selective processing of social stimuli in the superficial amygdala. Hum Brain Mapp. 30(10):3332-8.

34. Amunts K, Kedo O, Kindler M, Pieperhoff P, Mohlberg H, Shah NJ, Habel U, Schneider F, Zilles K (2005) Cytoarchitectonic mapping of the human amygdala, hippocampal region and entorhinal cortex: intersubject variability and probability maps. Anat Embryol (Berl) Dec;210(5-6):343-52.

35. Eickhoff SB, Heim S, Zilles K, Amunts K (2006) Testing anatomically specified hypotheses in functional imaging using cytoarchitectonic maps. Neuroimage. 32(2):570-82.

36. Ball T, Rahm B, Eickhoff SB, Schulze-Bonhage A, Speck O, Mutschler I (2007) Response properties of human amygdala subregions: evidence based on functional MRI combined with probabilistic anatomical maps. PLoS One. 2(3):e307.

37. Bzdok D, Laird AR, Zilles K, Fox PT, Eickhoff SB (2013) An investigation of the structural, connectional, and functional subspecialization in the human amygdala. Hum Brain Mapp 34(12):3247-66.

38. Belova MA, Paton JJ, Morrison SE, Salzman CD (2007) Expectation modulates neural responses to pleasant and aversive stimuli in primate amygdala. Neuron 55(6):970-84.

39. Rutledge RB, Dean M, Caplin A, Glimcher PW (2010) Testing the reward prediction error hypothesis with an axiomatic model. J Neurosci 30(40):13525-36.

40. Furmark T, Tillfors M, Marteinsdottir I, Fischer H, Pissiota A, Långström B, Fredrikson M (2002) Common changes in cerebral blood flow in patients with social phobia

treated with citalopram or cognitive-behavioral therapy. Arch Gen Psychiatry 59(5):425-33.

41. Etkin A, Wager TD (2007) Functional neuroimaging of anxiety: a meta-analysis of emotional processing in PTSD, social anxiety disorder, and specific phobia. Am J Psychiatry 164(10):1476-88.

42. Shackman AJ, Fox AS (2016) Contributions of the Central Extended Amygdala to Fear and Anxiety. J Neurosci. 36(31):8050-63.

43. Hendler T, Rotshtein P, Yeshurun Y, Weizmann T, Kahn I, Ben-Bashat D, Malach R, Bleich A (2003) Sensing the invisible: differential sensitivity of visual cortex and amygdala to traumatic context. Neuroimage 19(3):587-600.

44. Admon R, Lubin G, Rosenblatt JD, Stern O, Kahn I, Assaf M, Hendler T (2013) Imbalanced neural responsivity to risk and reward indicates stress vulnerability in humans. Cereb Cortex. 2013 23(1):28-35.

45. Grupe DW, Nitschke JB (2013) Uncertainty and anticipation in anxiety: an integrated neurobiological and psychological perspective. Nat Rev Neurosci 14(7):488-501.

46. Brierley B, Shaw P, David AS (2002) The human amygdala: a systematic review and meta-analysis of volumetric magnetic resonance imaging. Brain Res Brain Res Rev. 39(1):84-105.

47. McLean CP, Asnaani A, Litz BT, Hofmann SG (2011) Gender differences in anxiety disorders: prevalence, course of illness, comorbidity and burden of illness. J Psychiatr Res. 45(8):1027-35.

48. Alvarez RP, Chen G, Bodurka J, Kaplan R, Grillon C (2011) Phasic and sustained fear in humans elicits distinct patterns of brain activity. Neuroimage 55(1):389-400.

49. Choi JM, Padmala S, Pessoa L (2012) Impact of state anxiety on the interaction between threat monitoring and cognition. Neuroimage 59(2):1912-23.

50. Robinson OJ, Charney DR, Overstreet C, Vytal K, Grillon C (2012) The adaptive threat bias in anxiety: amygdala-dorsomedial prefrontal cortex coupling and aversive amplification. Neuroimage 60(1):523-9.

51. Klumpers F, Kroes MCW, Baas JMP, Fernández G (2017) How Human Amygdala and Bed Nucleus of the Stria Terminalis May Drive Distinct Defensive Responses. J Neurosci 37(40):9645-9656.

52. Romanski LM, LeDoux JE (1992) Equipotentiality of thalamo-amygdala and thalamo-cortico-amygdala circuits in auditory fear conditioning. J Neurosci 12(11):4501-9.

53. McDonald AJ (1998) Cortical pathways to the mammalian amygdala. Prog Neurobiol 55(3):257-332.

54. Bach DR, Behrens TE, Garrido L, Weiskopf N, Dolan RJ (2011) Deep and superficial amygdala nuclei projections revealed in vivo by probabilistic tractography. J Neurosci 31(2):618-23.

55. Dunsmoor JE, Bandettini PA, Knight DC (2008) Neural correlates of unconditioned response diminution during Pavlovian conditioning. **Neuroimage**. 1;40(2):811-817.

56. Knight DC, Waters NS, King MK, Bandettini PA (2010) Learning-related diminution of unconditioned SCR and fMRI signal responses. Neuroimage. 49(1):843-8.

57. Schiller D, Levy I, Niv Y, LeDoux JE, Phelps EA (2008) From fear to safety and back: reversal of fear in the human brain. J Neurosci 28(45):11517-25.

58. Roy M, Shohamy D, Daw N, Jepma M, Wimmer GE, Wager TD (2014) Representation of aversive prediction errors in the human periaqueductal gray. Nat Neurosci 17(11):1607-12.

59. Eippert F, Gamer M, Büchel C (2012) Neurobiological mechanisms underlying the blocking effect in aversive learning. J Neurosci 32(38):13164-76.

60. McNally GP, Johansen JP, Blair HT (2011) Placing prediction into the fear circuit. Trends Neurosci 34(6):283-92.

61. McHugh SB, Barkus C, Huber A, Capitão L, Lima J, Lowry JP, Bannerman DM (2014) Aversive prediction error signals in the amygdala. J Neurosci 34(27):9024-33.

62. Carlson JM, Greenberg T, Rubin D, Mujica-Parodi LR (2011) Feeling anxious: anticipatory amygdalo-insular response predicts the feeling of anxious anticipation. Soc Cogn Affect Neurosci 6(1):74-81.

63. Garfinkel SN, Minati L, Gray MA, Seth AK, Dolan RJ, Critchley HD (2014) Fear from the heart: sensitivity to fear stimuli depends on individual heartbeats. J Neurosci 34(19):6573-82.

64. Rauch SL, Whalen PJ, Shin LM, McInerney SC, Macklin ML, Lasko NB, Orr SP, Pitman RK (2000) Exaggerated amygdala response to masked facial stimuli in posttraumatic stress disorder: a functional MRI study. Biol Psychiatry 47(9):769-76.

65. Semple WE, Goyer PF, McCormick R, Donovan B, Muzic RF Jr, Rugle L, McCutcheon K, Lewis C, Liebling D, Kowaliw S, Vapenik K, Semple MA, Flener CR, Schulz SC (2000) Higher brain blood flow at amygdala and lower frontal cortex blood flow in PTSD patients with comorbid cocaine and alcohol abuse compared with normals. Psychiatry 63(1):65-74.

66. Sakai Y, Kumano H, Nishikawa M, Sakano Y, Kaiya H, Imabayashi E, Ohnishi T, Matsuda H, Yasuda A, Sato A, Diksic M, Kuboki T (2005) Cerebral glucose metabolism associated with a fear network in panic disorder. Neuroreport 16(9):927-31.

67. Brohawn KH, Offringa R, Pfaff DL, Hughes KC, Shin LM (2010) The neural correlates of emotional memory in posttraumatic stress disorder. Biol Psychiatry 68(11):1023-30.

68. Etkin A, Prater KE, Hoeft F, Menon V, Schatzberg AF (2010) Failure of anterior cingulate activation and connectivity with the amygdala during implicit regulation of emotional processing in generalized anxiety disorder. Am J Psychiatry 167(5):545-54.

69. Indovina I, Robbins TW, Núñez-Elizalde AO, Dunn BD, Bishop SJ (2011) Fear-conditioning mechanisms associated with trait vulnerability to anxiety in humans. Neuron 69(3):563-71.

70. Browning M, Behrens TE, Jocham G, O'Reilly JX, Bishop SJ (2015) Anxious individuals have difficulty learning the causal statistics of aversive environments. Nat Neurosci 18(4):590-6.

71. Grillon C (2002) Associative learning deficits increase symptoms of anxiety in humans. Biol Psychiatry 51(11):851-8.

72. Homan P, Levy I, Feltham E, Gordon C, Hu J, Li J, Pietrzak RH, Southwick S, Krystal JH, Harpaz-Rotem I, Schiller D (2019) Neural computations of threat in the aftermath of combat trauma. Nat Neurosci. 22(3):470-476.

73. Schönbrodt FD, Perugini M (2013) At what sample size do correlations stabilize? J Res Pers. 47:609-612.

74. Poldrack RA, Baker CI, Durnez J, Gorgolewski KJ, Matthews PM, Munafò MR, Nichols TE, Poline JB, Vul E, Yarkoni T (2017) Scanning the horizon: towards transparent and reproducible neuroimaging research. Nat Rev Neurosci. 18(2):115-126.

75. Rorden C, Brett M (2000) Stereotaxic display of brain lesions. Behav Neurol 12:191–200.

Figure legends

Figure 1. *Experimental task.*

At cue presentation, one of two insects (mosquito / bug) appeared next to a hand indexed an objective probability, learned before the scanning session, of an upcoming electrical shock. One insect indicated a high probability, and one insect indicated a low probability of receiving a shock. At outcome, an appearance of a red dot superimposed on the hand indicated receipt of concurrent shock. By contrast, a red dot next to the hand indicated no shock. Following a jittered fixation, subjects were asked to report how anxious they remembered feeling during cue presentations, i.e., whilst the insect had been present. After another jittered fixation, one of the two insects appeared again to indicate the beginning of the next trial.

Figure 2. *Amygdala responses to different levels of threat at cue presentation*

(A) Greater BLA activity at time of cue presentation was associated with enhanced objective threat levels, i.e., high vs. low probability of upcoming shock.

(B) Trend-level interaction between 'subregion' and 'expectation' at cue, with significant threat modulation (high vs. low probability of upcoming shock) in BLA, and no effect in CMA. Mean betas for bilateral BLA and CMA masks. * p<0.05, (*) p=0.074, n.s. = not significant, a.u. = arbitrary units, error bars indicate SEM. Neural results are presented as SPM activation maps overlaid on a default structural brain in MRIcron (75).

Figure 3. *Dissociation between BLA and CMA in response to aversive events*

(A) Shock vs. no shock outcomes are associated with increased outcome-related activity in the CMA.

(B) Low vs. high expectation cue are associated with increased activity in the BLA at the time of outcomes, contrasting with expectation-related modulation at the time of cue presentation.

(C) Response to all four outcome types in CMA: Activity in CMA represents aversive events, which are not modulated by expectations. Mean betas for bilateral CMA mask. High & Low = high and low probability of shock.

(D) Response to all four outcome types in BLA. Activity in BLA represents an aversive prediction error that depends on both aversive events and expectations about those events. Stronger activation for less predicted (low probability of shock) as compared to highly predicted (high probability of shock) aversive events. Stronger attenuation of responses for

less predicted (high probability of shock) as compared to highly predicted (low probability of shock) omission of aversive events. Mean betas for bilateral BLA mask. High & Low = high and low probability of shock.

(E) Significant interaction between subregion and outcome as indicated by greater shock responses in CMA than BLA. Significant interaction between subregion and expectation as indicated by significant effect of expectation in BLA, and no effect in CMA. Mean betas for bilateral BLA and CMA masks. *** p<0.001, ** p<0.01, * p<0.05, n.s. = not significant, a.u. = arbitrary units, error bars indicate SEM.

Figure 4. *Amygdala activity and subjective aversive experience*

(A) Subjective reports of remembered anticipatory anxiety at cue presentation. Anxiety ratings were influenced by both objective threat level in the cue period, i.e., greater for high vs. low expectation of upcoming shock, and were also biased by experienced outcomes, i.e., greater for shock vs. no shock trials, error bars indicate SEM.

(B) A greater neural difference between cue-elicited BLA responses (high vs. low probability of upcoming shock) was linked to a greater dissociation between threat levels in anxiety ratings (high vs. low probability of shock). * p<0.05, a.u. = arbitrary units.

(C) Positive correlation between trial-by-trial variability in CMA activity at time of reporting on a visual analogue scale and retrospective reports of subjective anxiety at cue presentation.
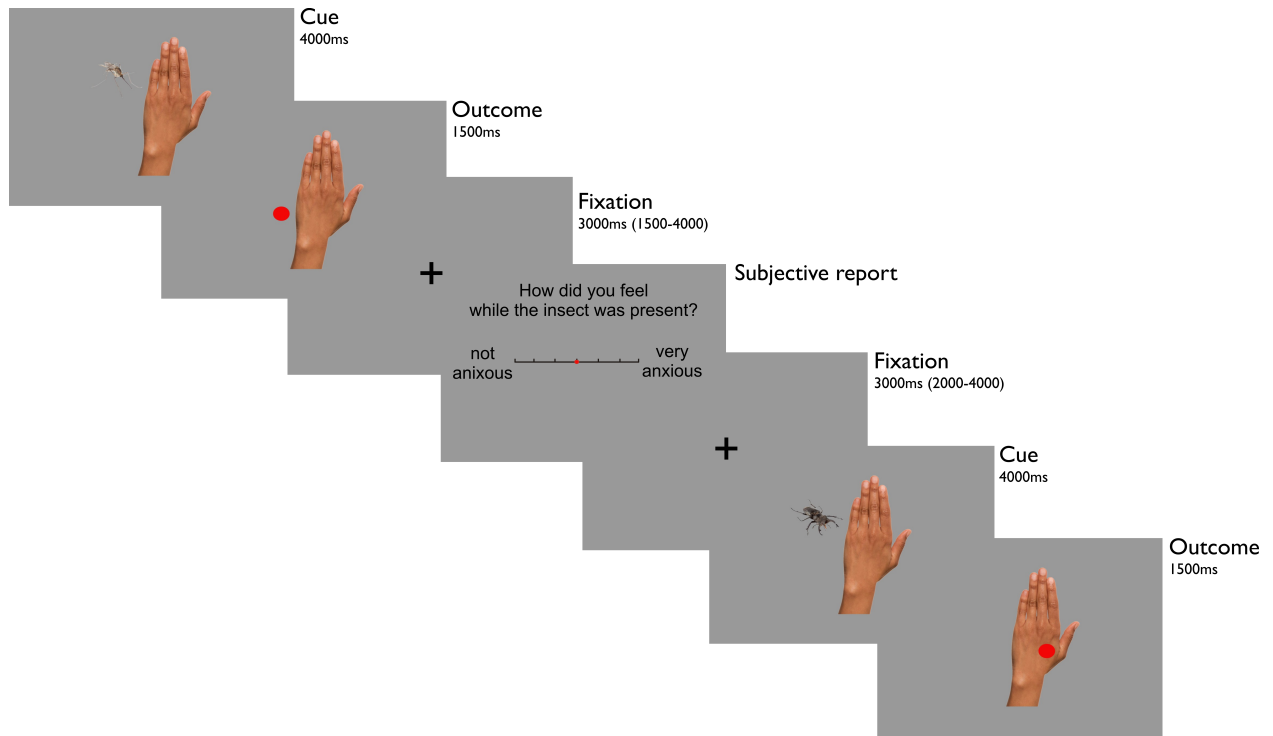
Figure 5. *Threat signals in BLA and trait anxiety*

(A) A greater overall cue-related BLA response (high *and* low probability of upcoming shock) was associated with greater trait anxiety.
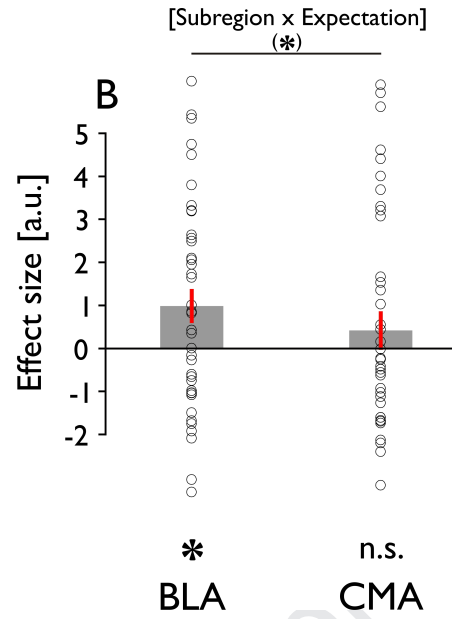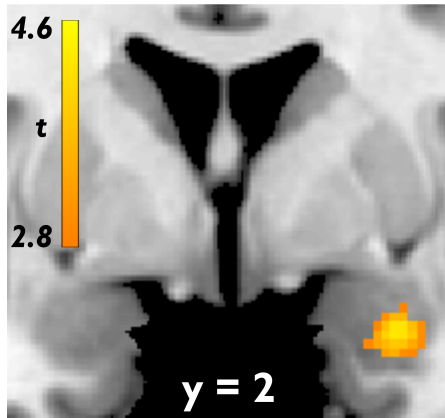
(B) A greater neural difference between cue-related BLA responses (high vs. low probability of upcoming shock) was associated with lower trait anxiety. * p<0.05, a.u. = arbitrary units.
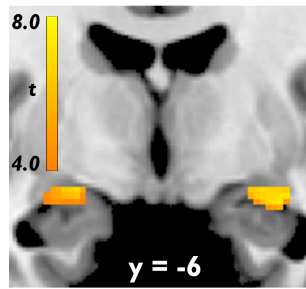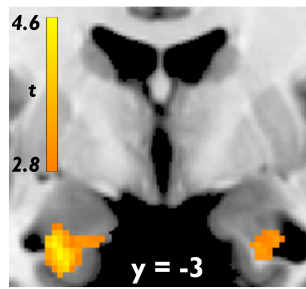
Cue
4000ms

Outcome
1500ms

Fixation
3000ms (1500-4000)

Subjective report

How did you feel
while the insect was present?

not
anixous

very
anxious

Fixation
3000ms (2000-4000)

Cue
4000ms

Outcome
1500ms

A Threat modulation in BLA
(High vs. low probability at cue)

4.6

t

2.8

y = 2

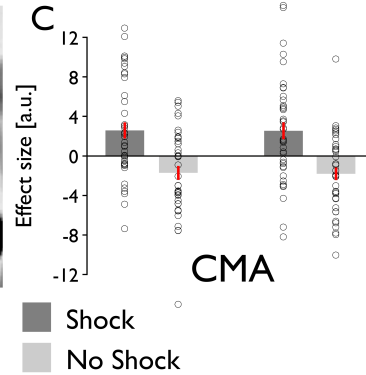**B** [Subregion x Expectation]
(∗)

Effect size [a.u.]

∗
BLA

n.s.
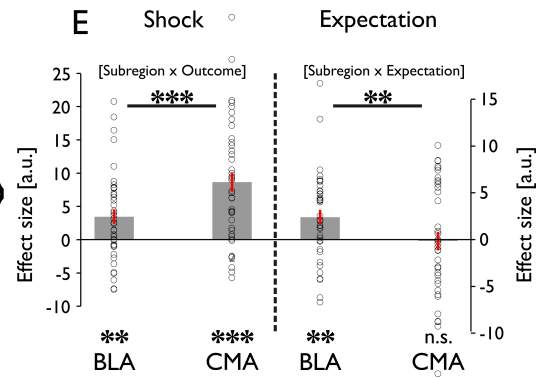CMA
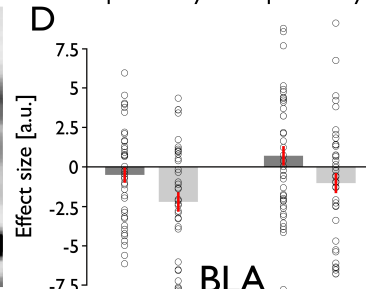
A Shock signals in CMA
(Shock vs. no shock at outcome)

B Expectation signals in BLA
(Low vs. high probability at outcome)

A

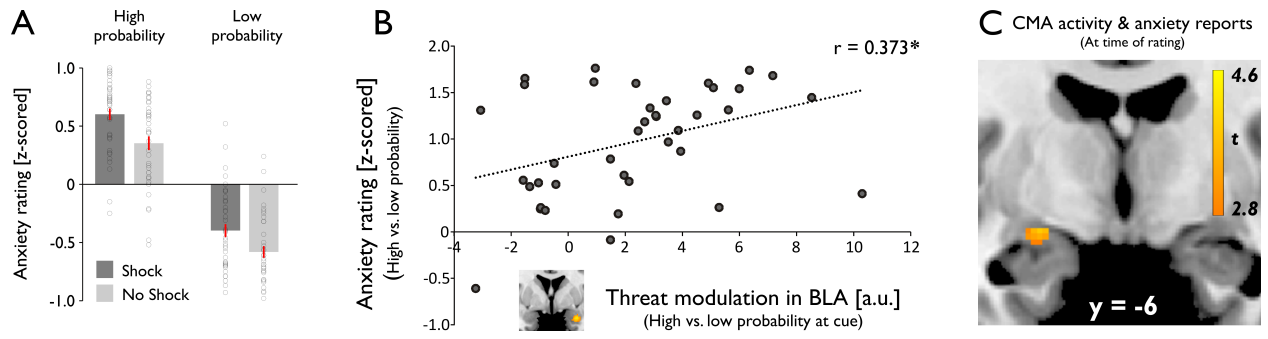High probability   Low probability

Anxiety rating [z-scored]

Shock
No Shock

B

Anxiety rating [z-scored]
(High vs. low probability)

r = 0.373*

Threat modulation in BLA [a.u.]
(High vs. low probability at cue)

C CMA activity & anxiety reports
(At time of rating)

t

y = -6

A Elevated threat response in anxiety

r = 0.328*

Trait Anxiety (High / Low)

Overall threat response in BLA [a.u.]
(High & low probability at cue)

B Undifferentiated threat modulation in anxiety

r = -0.322*

Trait Anxiety (High / Low)

Threat modulation in BLA [a.u.]
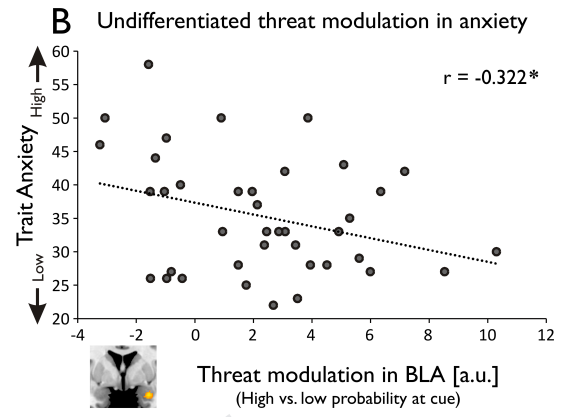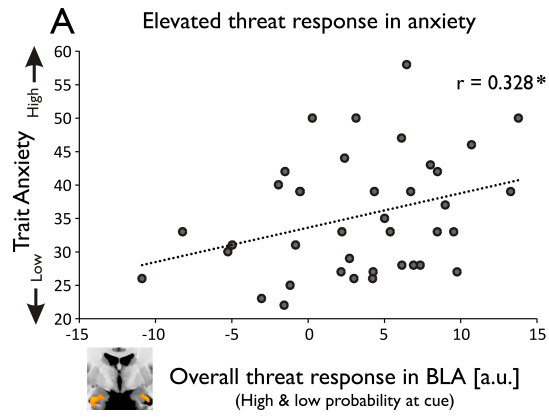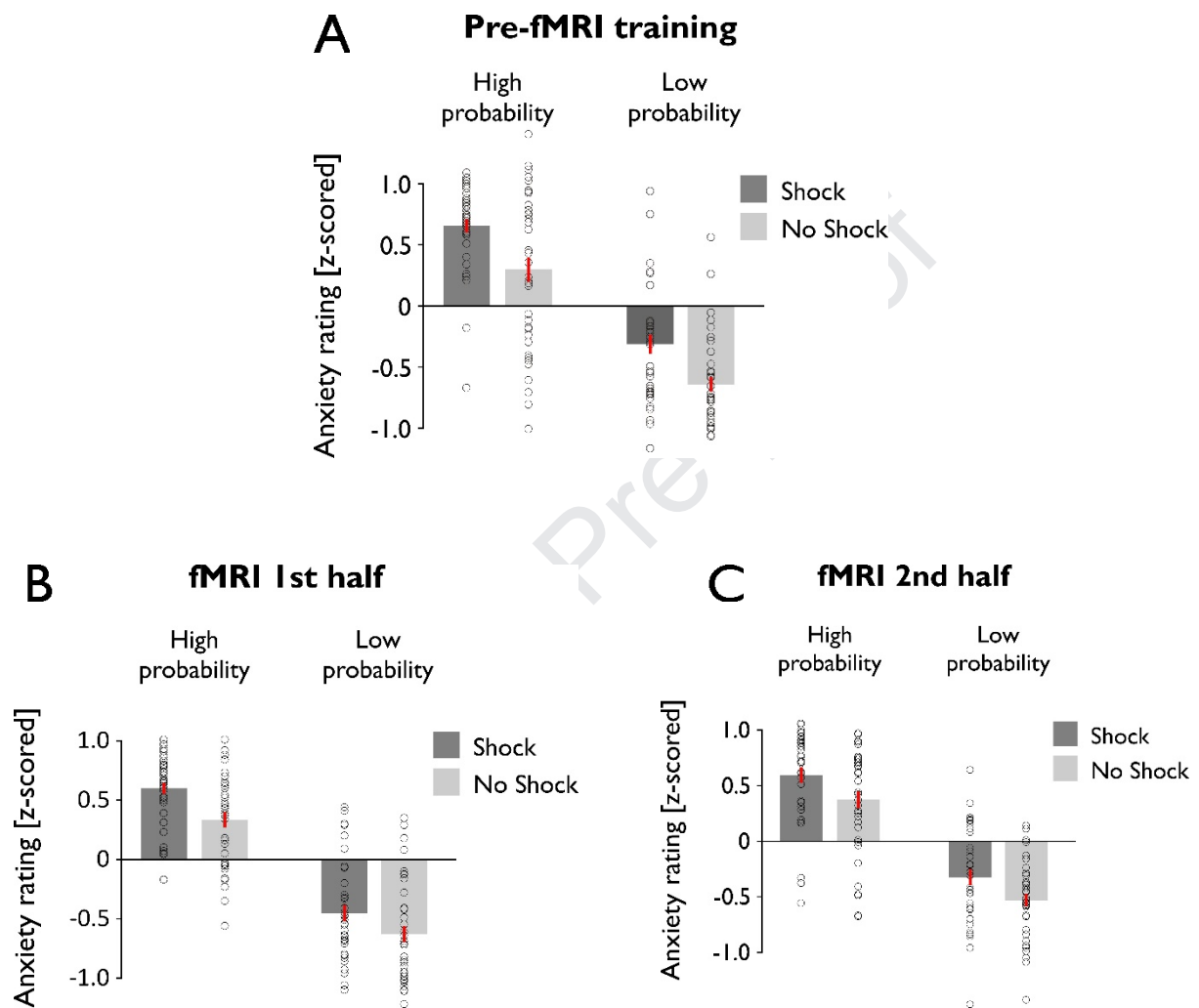(High vs. low probability at cue)

Distinct Processing of Aversive Experience in Amygdala Subregions

Supplementary Information

Supplementary Figure S1. *Anxiety ratings for pre-fMRI training and 1st and 2nd half of the fMRI experiment.* Subjective reports of remembered anticipatory anxiety at cue presentation. Anxiety ratings were influenced by both objective threat level in the cue period, i.e., greater for high vs. low expectation of upcoming shock, and were also biased by experienced outcomes, i.e., greater for shock vs. no shock trials. Error bars indicate SEM.

(A) Subjects had already learned to dissociate between two threat levels during training, as indicated by strong main effect of 'expectation' (high vs. low probability) [$F_{(1,38)}=74.730$, $p<0.001$]. Similar to the main experiment, we also found a significant main effect of 'outcome' (shock vs. no shock) [$F_{(1,38)}=23.621$, $p<0.001$], with no interaction [$F_{(1,38)}=0.064$, $p=0.802$].

(B) & (C) Similar results were found when splitting the fMRI experiment in two separate halves:

1st half: 'expectation' (high vs. low probability): [$F_{(1,38)}=109.074$, $p<0.001$], 'outcome' (shock vs. no shock): [$F_{(1,38)}=23.828$, $p<0.001$], interaction: [$F_{(1,38)}=2.499$, $p=0.122$].

2nd half: 'expectation' (high vs. low probability): [$F_{(1,38)}=73.052$, $p<0.001$], 'outcome' (shock vs. no shock): [$F_{(1,38)}=15.149$, $p<0.001$], interaction: [$F_{(1,38)}=0.311$, $p=0.588$].

	Entire Amygdala			BLA					CMA					BLA vs CMA
	voxel			voxel			mask		voxel			mask		mask
	[x y z]	T=	P_FWE=	[x y z]	T=	P_FWE=	beta=	P=	[x y z]	T=	P=	beta=	P=	P=
Cue														
Expectation														
6mm	29 2 -23	4.17	0.028	29 3 -24	4.47	0.018	0.986	0.017	-	-	-	0.416	0.357	0.074
4.5mm	29 2 -21	4.30	0.024	29 3 -24	4.38	0.027	1.000	0.019	-	-	-	0.384	0.426	0.088
3mm	27 2 -20	4.54	0.019	27 2 -21	4.09	0.080	0.939	0.029	-	-	-	0.370	0.456	0.156
Outcome														
Shock														
6mm	26 -9 -12	8.28	<0.001	26 3 -21	5.83	<0.001	3.441	0.003	26 -9 -12	7.07	<0.001	8.662	<0.001	<0.001
	-20 -6 -12	7.20	<0.001	-24 -2 -20	4.79	0.007			-20 -6 -12	7.20	<0.001			
4.5mm	26 -9 -12	8.38	<0.001	26 3 -20	5.32	0.002	3.044	0.009	26 -8 -12	6.87	<0.001	9.222	<0.001	<0.001
	-24 -8 -12	6.80	<0.001	-24 -2 -20	4.69	0.011			-24 -8 -12	6.80	<0.001			
3mm	26 -9 -12	7.80	<0.001	24 3 -18	4.82	0.012	2.902	0.011	26 -6 -12	5.98	<0.001	9.790	<0.001	<0.001
	-26 -8 -12	7.15	<0.001	-24 -2 -20	4.52	0.026			-26 -9 -12	6.33	<0.001			
Expectation														
6mm	-27 -2 -26	4.41	0.016	-26 -2 -30	4.44	0.020	2.402	0.003	-	-	-	-0.138	0.886	0.003
4.5mm	-26 -3 -29	3.78	0.086	-26 0 -32	4.06	0.060	2.475	0.002	-	-	-	-0.276	0.796	0.005
3mm	30 -2 -24	3.86	0.102	-27 -5 -26	4.09	0.081	2.593	0.001	-	-	-	-0.335	0.779	0.009
VAS														
Self-reports														
6mm	-23 -6 -12	4.14	0.032	-	-	-	0.918	0.611	-23 -6 -12	4.14	0.011	4.125	0.032	0.014
4.5mm	-24 -5 -12	4.03	0.050	-	-	-	0.854	0.642	-24 -5 -14	3.94	0.021	4.237	0.047	0.021
3mm	-24 -5 -12	3.95	0.088	-	-	-	0.821	0.660	-24 -5 -14	3.86	0.034	4.223	0.078	0.045

Supplementary Table S1. *Main results for different smoothing kernels*
The main results reported in the manuscript (6mm smoothing kernel), as assessed with 4.5mm and 3mm smoothing kernels, respectively. Results are shown at the voxel-level (x, y, z coordinates in MNI-space), FWE-corrected for the respective bilateral mask, and for mean activation across the bilateral masks.
Cue Expectation: Activity at time of cue presentation for high vs. low probability of upcoming shock., Outcome Shock: Activity at time of outcome presentation for shock vs. no shock., Outcome Expectation: Activity at time of outcome presentation for low vs. high probability of shock., VAS Self-reports: Positive correlation between trial-by-trial activity at time of reporting and retrospective reports of subjective anxiety at cue presentation.
Entire amygdala = Independent bilateral amygdala mask from WFU PickAtlas toolbox, defined using the Automated Anatomical Labelling (AAL), CMA = Bilateral centromedial amygdala mask, BLA = Bilateral basolateral amygdala mask.
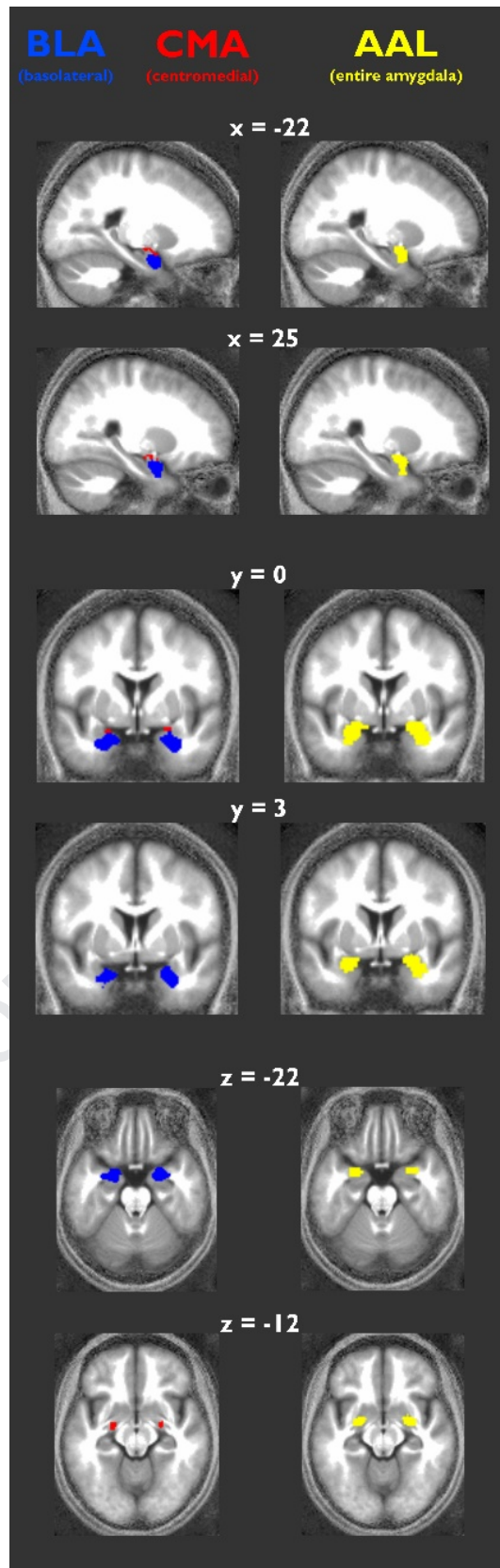
	Entire Amygdala					BLA				CMA			
	[x y z]	T=	P_FWE=	% BLA	% CMA	[x y z]	T=	P_FWE=	% BLA	[x y z]	T=	P_FWE=	% CMA
Cue													
Expectation	29 2 -23	4.17	0.028	37 [21-58]	0	29 3 -24	4.47	0.018	37 [18-57]	-	-	-	-
Outcome													
Shock	26 -9 -12	8.28	<0.001	0	19 [5-33]	26 3 -21	5.83	<0.001	40 [30-51]	26 -9 -12	7.07	<0.001	19 [5-33]
	-20 -6 -12	7.20	<0.001	0	36 [14-42]	-24 -2 -20	4.79	0.007	33 [23-55]	-20 -6 -12	7.20	<0.001	36 [14-42]
Expectation	-27 -2 -26	4.41	0.016	91 [58-94]	0	-26 -2 -30	4.44	0.020	85 [64-90]	-	-	-	-
VAS													
Self-reports	-23 -6 -12	4.14	0.032	0	31 [12-39]	-	-	-	-	-23 -6 -12	4.14	0.011	31 [12-39]

Supplementary Table S2. *Peak voxel statistics and cytoarchitectonic probabilities*
Results are shown at the voxel-level (x, y, z coordinates in MNI-space), p-values represent FWE-corrected statistics for the respective bilateral mask. Probabilities are computed from maximum probability maps, i.e., summary maps of different probabilistic cytoarchitectonic maps as implemented in the SPM anatomy toolbox.
Cue Expectation: Activity at time of cue presentation for high vs. low probability of upcoming shock., Outcome Shock: Activity at time of outcome presentation for shock vs. no shock., Outcome Expectation: Activity at time of outcome presentation for low vs. high probability of shock., VAS Self-reports: Positive correlation between trial-by-trial activity at time of reporting and retrospective reports of subjective anxiety at cue presentation.
Entire amygdala = Independent bilateral amygdala mask from WFU PickAtlas toolbox, defined using the Automated Anatomical Labelling (AAL), CMA = Bilateral centromedial amygdala mask, BLA = Bilateral basolateral amygdala mask.

Supplementary Figure S2. *Visualisation of the ROIs superimposed on the mean normalized structural image.* CMA: Centromedial amygdala & BLA: Basolateral amygdala as derived from the SPM anatomy toolbox. AAL: Independent entire amygdala mask from WFU PickAtlas toolbox, defined using the Automated Anatomical Labelling (AAL) atlas. x, y, z coordinates in MNI-space.

4
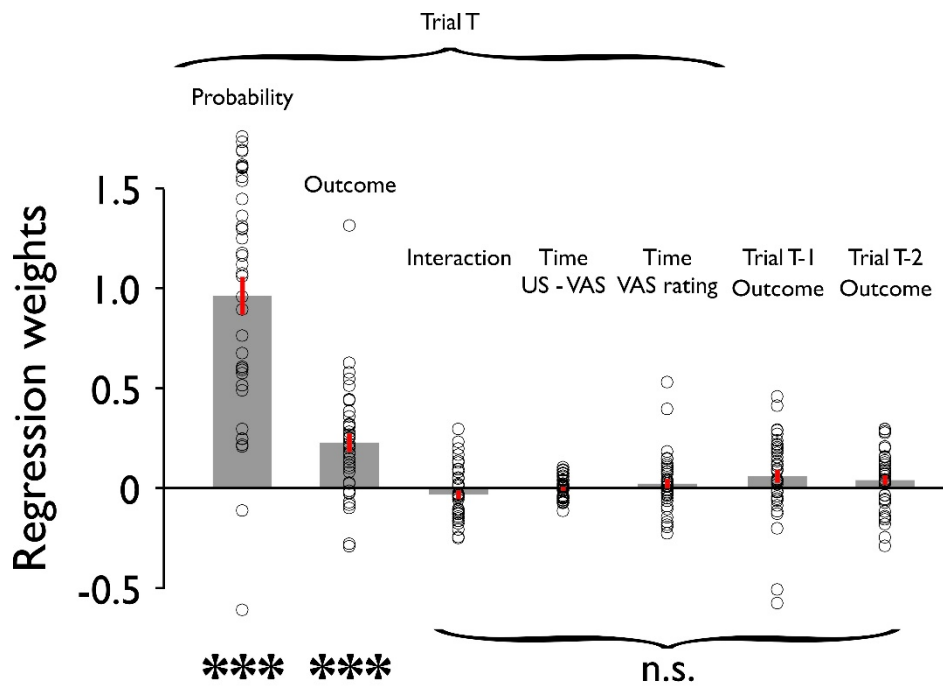
Supplementary Figure S3. *Trial-by-trial regression model of subjective anxiety ratings.*
To predict anxiety ratings on current trial T, we used (i) probability (high vs. low), (ii) outcome type (shock vs. no shock), and (iii) interaction term of the current trial T, whilst also testing for influence of (iv) elapsed time since outcome receipt (Time US-VAS), (v) time taken to report (Time VAS rating) and outcome type of previous trials, i.e., (vi) Trial T-1 and (vii) T-2.
Results confirmed the average effects reported in the manuscript:
Effect of probability (i): p<0.001; Effect of outcome (ii): p<0.001: Interaction n.s.: p=0.131, whilst additionally showing no effects of (iv): p=0.720, (v): p=0.331; (vi): p=0.074; (vii): p=0.091.
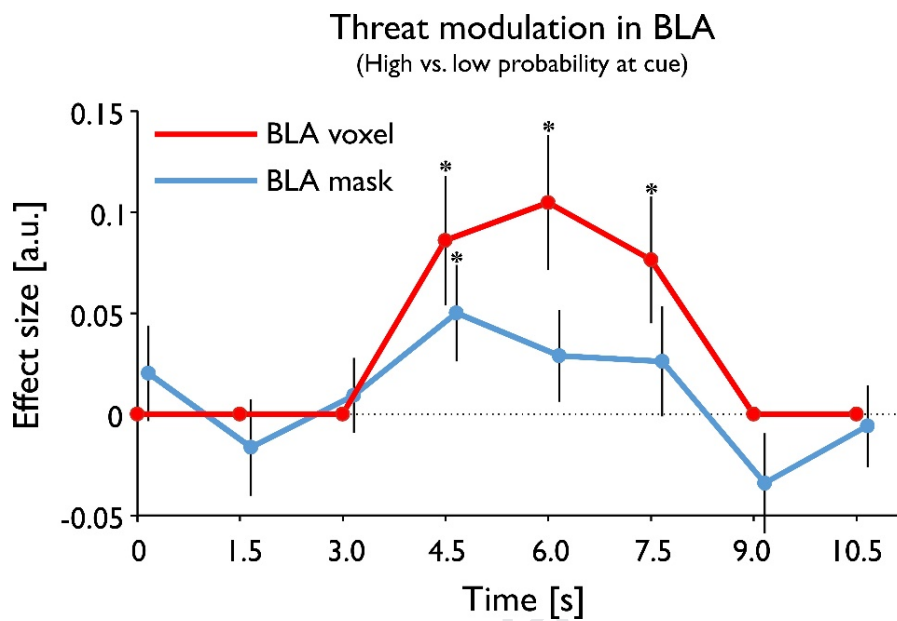
Supplementary Figure S4. *Finite impulse response analysis.*
BOLD response to aversive cues was modelled with a finite impulse response set consisting of a number of successive post-stimulus time bins ("mini-boxcars", 1.5s). Here, time represents post-stimulus onset time in seconds. This analysis revealed that BOLD response to threat, i.e., high vs. low probability at cue, showed a response pattern remarkably similar to a canonical HRF, with peak activity around 5-6s post-stimulus onset (as predicted by a canonical HRF). Note that this was true for both BLA peak voxel (informed from our conventional analysis, $p<0.05$) and mean activity averaged across the entire bilateral BLA mask.
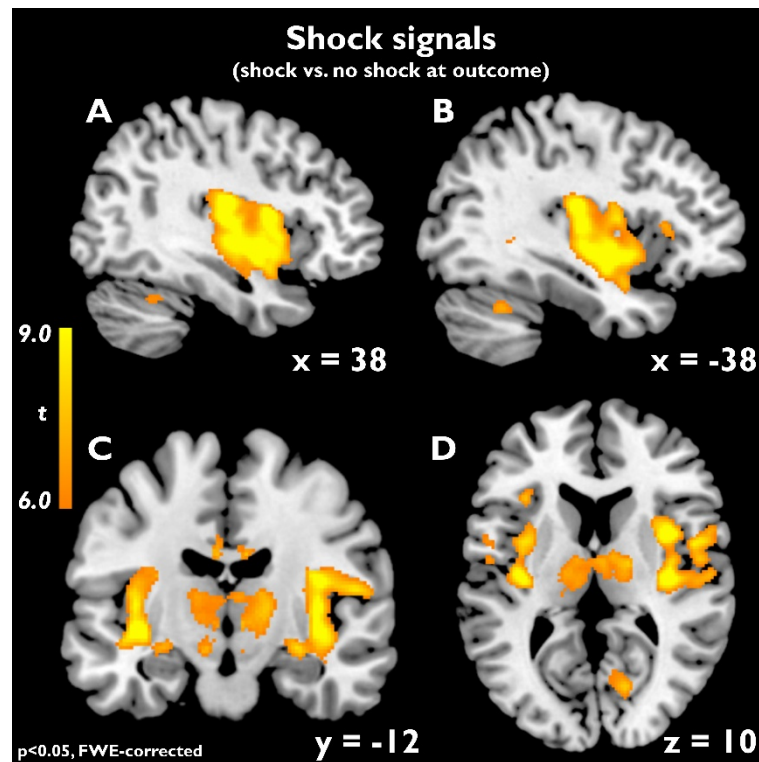
Supplementary Figure S5. *Whole-brain shock signals*
Contrast shock vs. no shock at outcome, $P_{FWE}<0.05$, whole-brain, corrected at voxel level.
x, y, z coordinates in MNI-space.
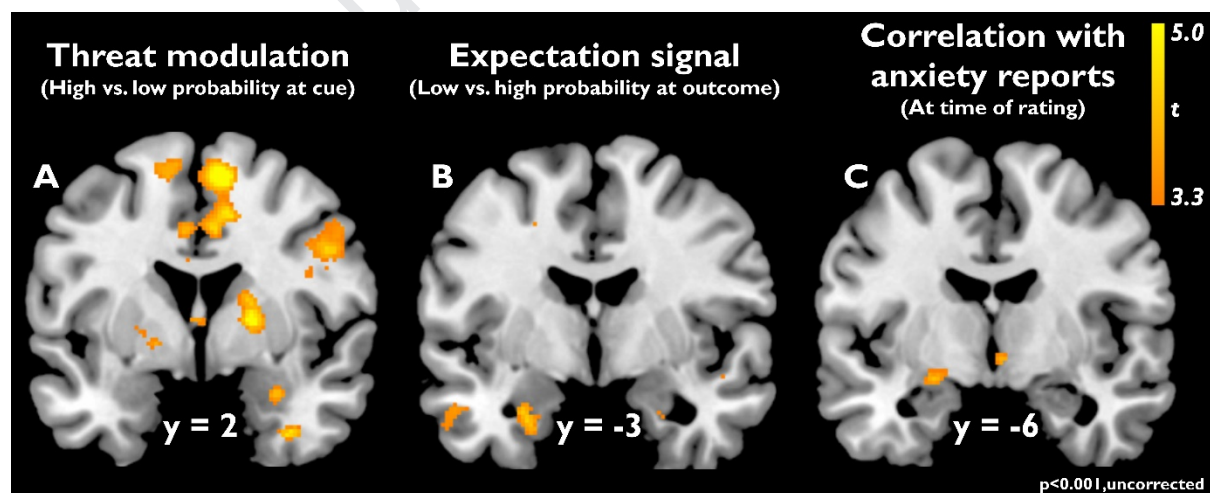
Supplementary Figure S6. *Whole-brain results at uncorrected height threshold, p<0.001.*
(A) Contrast high vs. low probability at cue.
(B) Contrast low vs. high probability at outcome.
(C) Positive correlation between trial-by-trial variability in activity at time of reporting on a visual analogue scale and retrospective reports of subjective anxiety at cue presentation.
Note that these slices correspond to the respective masked amygdala results presented in the main manuscript.
x, y, z coordinates in MNI-space.

Region	[x y z]	T=	P_FWE=
Primary Sensory Cortex (SI) – Right	38 -15 18	12.72	<0.001
Insula – Left	-36 -18 17	12.46	<0.001
Insula – Right	38 -2 -8	11.64	<0.001
Secondary Sensory Cortex (SII) – Right	56 -17 14	10.43	<0.001
Secondary Sensory Cortex (SII) – Left	-59 -26 24	9.11	<0.001
Precuneus – Left	-6 -69 33	8.94	<0.001
Periaqueductal Gray (PAG) – Left	-8 -27 -8	8.83	<0.001
Periaqueductal Gray (PAG) – Right	6 -30 -15	8.45	<0.001
Primary Sensory Cortex (SI) – Left	-47 -21 23	8.42	<0.001
Posterior Cingulate Cortex (PCC) – Left	-6 -21 30	8.32	<0.001
Thalamus – Right	8 -5 8	8.31	<0.001
Inferior Frontal Gyrus (IFG) – Left	-27 35 -14	7.83	0.001
Visual Cortex – Right	15 -72 11	7.83	0.001
Cerebellum – Right	6 -56 -35	7.73	0.001
Insula – Right	-35 23 12	7.64	0.002
Cerebellum – Right	2 -74 -15	7.62	0.002
Thalamus – Left	-14 -17 5	7.38	0.004
Middle Cingulate Cortex (MCC) – Right	5 18 35	7.28	0.006
Posterior Cingulate Cortex (PCC) – Left	-5 -41 41	7.25	0.006
Cerebellum – Left	-39 -54 -30	7.22	0.007
Centromedial Amygdala (CMA) – Left	-20 -6 -12	7.20	0.007
Visual Cortex – Left	-3 -83 6	7.17	0.008
Centromedial Amygdala (CMA) – Right	26 -9 -12	7.07	0.012
Anterior Cingulate Cortex (ACC) – Left	-5 18 30	7.05	0.012
Inferior Frontal Gyrus (IFG) – Right	33 32 5	6.53	0.048

Supplementary Table S3. *Whole-brain shock signals (corresponding to Supplementary Fig. 4)*
Local maxima derived from the contrast shock vs. no shock at outcome.
P_FWE<0.05, whole-brain, corrected at voxel level.
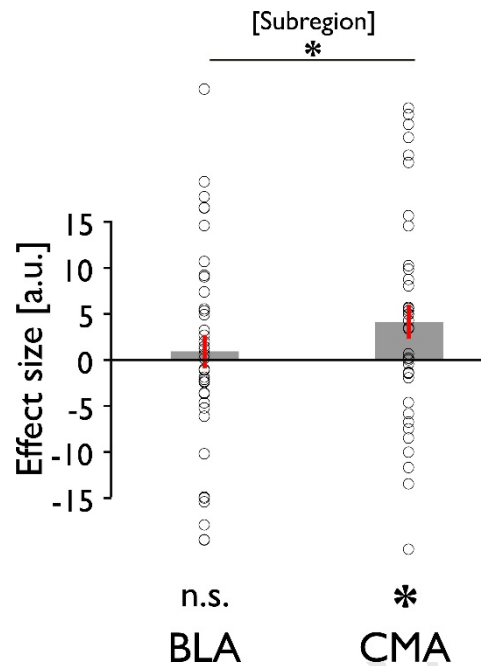
Supplementary Figure S7. *Relationship between activity at time of reporting and subjective anxiety.*
Mean betas for bilateral BLA and CMA masks for positive correlation between trial-by-trial-variability in activity and retrospective anxiety reports. * p<0.05, n.s. = not significant, a.u. = arbitrary units, error bars indicate SEM.
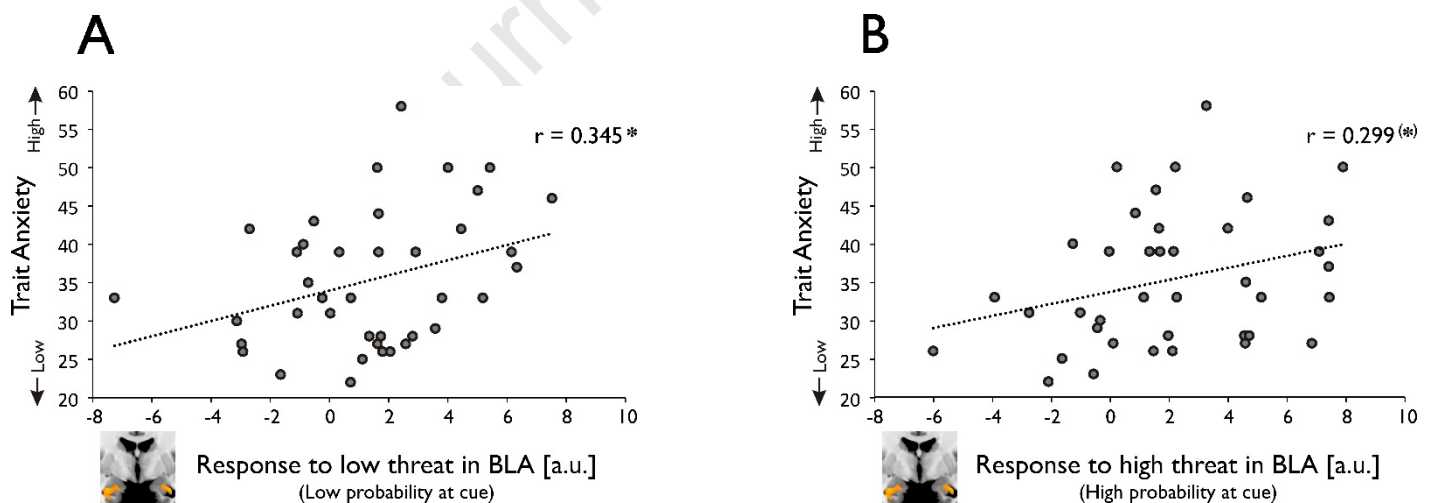
Supplementary Figure S8. *Threat signals in BLA and trait anxiety*
A greater cue-related BLA response to low (A) and (B) high levels of threat was associated with greater trait anxiety.
* p<0.05, (*) p=0.064; a.u. = arbitrary units.
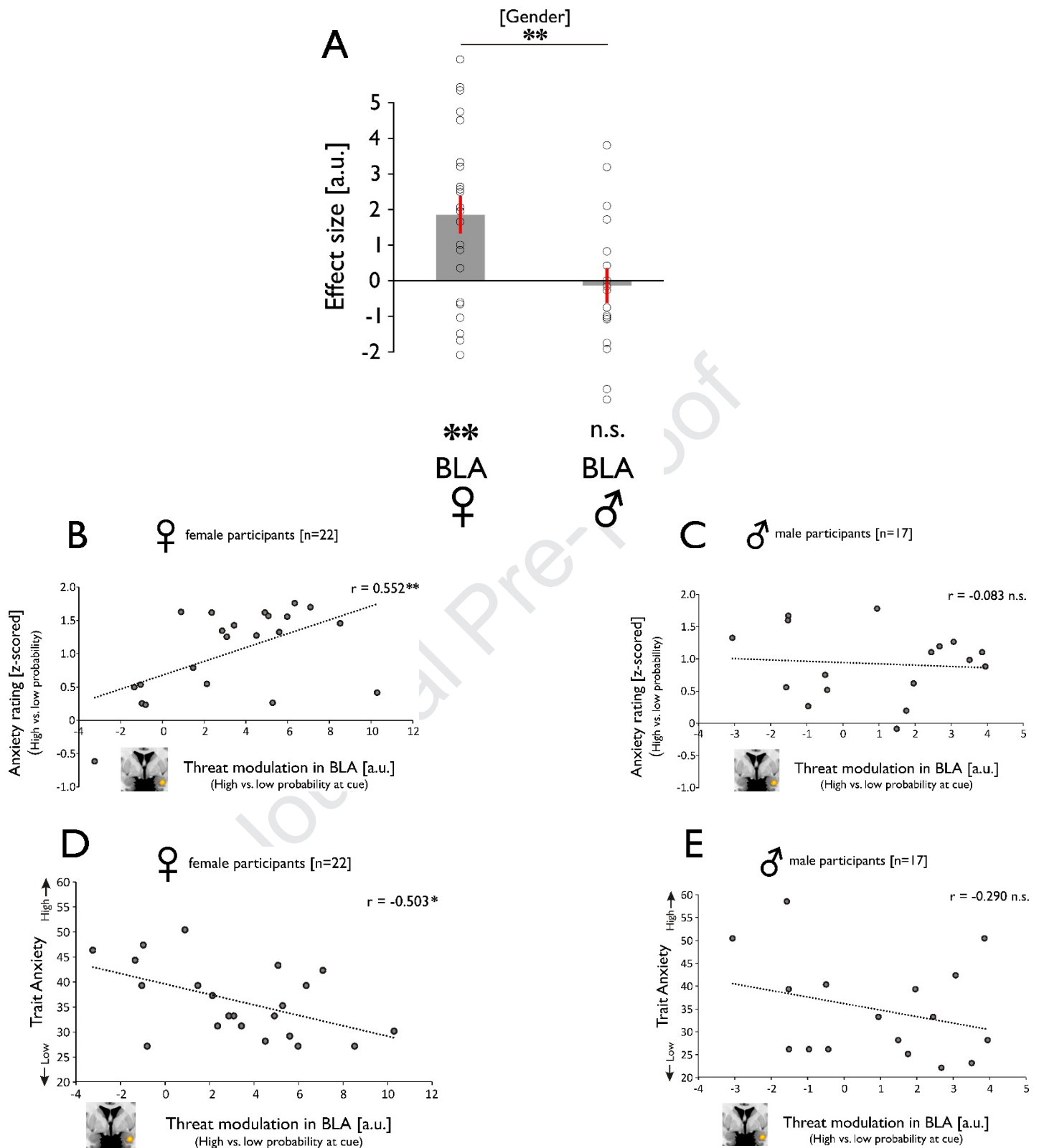
Supplementary Figure S9. *Sex differences in BLA threat modulation.*
(A) BLA activity at time of cue presentation scaling with enhanced objective threat levels, i.e., high vs. low probability of upcoming shock was significantly greater in female than male participants.
A greater neural difference between cue-elicited BLA responses (high vs. low probability of upcoming shock) was linked to a greater dissociation between threat levels in anxiety ratings (high vs. low probability of shock) in female (|B) but not in male participants (C). A greater neural difference between cue-related BLA responses (high vs. low probability of upcoming shock) was associated with lower trait anxiety in female (|D) but not in male participants (E). ** p<0.01, * p<0.05, n.s. = not significant, a.u. = arbitrary units, error bars indicate SEM.